Polymer(Korea), Vol. 42, No. 6, pp. 901-909 (2018)
https://doi.org/10.7317/pk.2018.42.6.901

ISSN 0379-153X(Print)
ISSN 2234-8077(Online)

FKM과의 혼합을 이용한 복합체 처리 향상 및 PVDF/FKM/CB의 특성과 전기전도성과의 관계

Mojtaba Deilamy Moezzi†, Mohammad Karrabi, and Yousef Jahani
Iran Polymer and Petrochemical Institute
(2018년 2월 21일 접수, 2018년 4월 7일 수정, 2018년 4월 17일 채택)

Improving on Processing of Composites via Blending with FKM and Relation between Electrical Conductivity and Properties of PVDF/FKM/CB

Mojtaba Deilamy Moezzi†, Mohammad Karrabi, and Yousef Jahani
Iran Polymer and Petrochemical Institute, P.O. Box 14965/115, Tehran, I.R. Iran
(Received February 21, 2018; Revised April 7, 2018; Accepted April 17, 2018)

Abstract: The present work was focused on studying the effects of different carbon black (CB) loadings on rheological, thermal, tensile, dynamic mechanical, and electrical properties of polyvinylidene fluoride (PVDF) and FKM composites. To these ends, dynamic mechanical analysis (DMA) was conducted, and the CB grade and method of compound preparation which was CB(N330) by melt mixing with different shear effects were examined. The composites were melting blended with CB at 190°C in an internal mixer. After that the properties of filled and unfilled composites were compared. DMA showed the glass transition temperatures of the composites. The analysis also revealed that the area under the loss tangent (tanδ) peak decreased; moreover the tanδ temperature of the rubber phase increased by CB loading. The presence of CB improved the mechanical properties, such as Young's modulus and tensile strength, of the composites and increased their thermal stability due to high thermal stability of CB and the interaction between CB particles and polymer matrix. The increase in the electrical conductivities of the composites under different CB loadings was also examined with different shear effects owing to different dispersion states of CB. The percolation threshold of conductive thermoplastic vulcanizate composite was observed based on conductive CB and the experimental data were well fitted to the general equation model(GEM).

Keywords: composites, poly(vinylidene fluoride), fluoroelastomer, carbon black.

Introduction

In recent years, polymer composites and polymer blends have been used extensively in various applications. Addition of filler into polymeric matrix and blending of polymers are well-established ways to improve the properties which cannot be achieved from the individual component. It is an effective cost and economic approach to produce a new material with desired properties.[1-3] However, the difference in molecular structure and affinity of blend component results in the immiscible blend. This has been recognized to cause both inferior mechanical properties such as poor tensile strength, elongation at break and compression set.[4,5] The blending of polymer has been studied extensively over the past decades in order to achieve a set of desired properties and high performances for specific applications.[6,7] The thermoplastic elastomeric combination is an interesting and new class of material, so-called "Thermoplastic Elastomer" (TPE). The TPE consists of a rigid thermoplastic phase and a soft elastomer phase, resulting in a combination of the excellent elastic properties of rubber with melt process ability of thermoplastic. The properties of TPE based on plastic-rubber blend depend on phase morphology and miscibility between two phases, mainly due to phase separation of the blend. There are two types of blending technique to prepare TPE: simple blend and dynamic vulcanization. The simple blend (SB) means blending of plastic and rubber without cross-linker.[8,9] The dynamic vulcanization is a blend with cross-linker to vulcanize rubber phase during melt mixing. The

†To whom correspondence should be addressed.
m.deilami@ippi.ac.ir

thermoplastic elastomer prepared by dynamic vulcanization is usually called thermoplastic vulcanizate (TPV).[10,11] Thermoplastic vulcanizates (TPVs) are prepared by a dynamic vulcanization technique by adding curative during a mixing operation. The TPVs consist of dispersion of vulcanized rubber domains in thermoplastic matrix, which differs from the simple blends. The viscosity plays a significant role on formation of TPV morphology. When the degree of vulcanization is high, the rubber particles may be broken into micron size of elastomeric particles. The dynamic vulcanization of rubber phase in the plastic matrix leads to formation of materials with improved properties of high elasticity, while thermoplastic phase provides the melt processing. The varieties of TPVs have already found commercial applications, especially in the automotive sector.[12,13]

Poly(vinylidene fluoride), or poly(1,1-difluoroethylene) is known by its acronym PVDF. Polymerization procedures, temperatures, pressure, recipe ingredients, monomer feeding strategy, and post polymerization are variables influencing product characteristics and quality.[14] In general, fluoropolymers are thermally more stable than hydrocarbon polymers. The high electronegativity of fluorine atoms on the chain and the high bond dissociation energy of the C–F bond provide the high stability of the fluoropolymers. PVDF has been observed to experience degradation during high-temperature operations. The outstanding heat stability and excellent oil resistance of these materials are due to the high ratio of fluorine to hydrogen, the strength of the carbon-fluorine bond, and the absence of unsaturation. PVDF generally possesses distinction chemical stability against most of the chemicals, including a wide range of harsh chemicals, inorganic acids and solvents.[15,16]

Fluoroelastomers (FKM) are a class of synthetic rubber which provide extraordinary levels of resistance to heat, oil and chemicals, while providing useful service life above 200 °C. FKM are a family of fluoropolymer rubbers, not a single entity. FKM can be classified by their fluorine content, 66%, 68%, and 70%, respectively. FKM having higher fluorine content have increasing fluids resistance derived from increasing fluorine levels.[17,18] One of these FKM, Viton A, is a copolymer of vinylidene fluoride (VDF) and hexafluoropropylene (HFP) developed by DuPont and was made available commercially in 1955. Many other reports have focused on chemical degradation of FKM rubbers in specific aggressive aqueous chemical environments. Many reports have been published on thermal degradation properties of FKMs, where attempts have been made to establish degradation mechanisms.[19,20]

Carbon black (CB) is a reinforcing filler and also widely used as conductive filler to improve mechanical and electrical properties of high-performance rubber materials. Different types of CB offer differences in mechanical and electrical properties which mainly depend on the specific surface area and/or structure of the primary aggregates.[21] An important characteristic of CBs is the diameter of the primary particles which is extremely small (typically less than 300 nm), in particular CBs, may even be up to 500 nm. The other characteristic feature is the CB structure. CBs are variously described as “low structure” and “high structure” that correlate with their spatial extent, the former having larger dimensions than the latter. The CB characterized by primary aggregates composed of many prime particles, with considerable branching and chaining, is referred to as a high-structure CB. If the primary aggregates consist of relatively few prime particles, the CB is referred to as a low-structure CB. The reinforcing potential in rubber is mainly attributed to two effects: (i) the formation of a physically bonded flexible filler network and (ii) strong polymer filler couplings. Both of these effects refer to a high surface activity and specific surface of the filler particles.[19] The fillers covered by the immobilized rubber interface can be considered as physical cross-links. This provides network chains for the rubber matrix in the proximity of CB particles.[22-24]

PVDF and FKM have partially similar physical properties. As one of the special functional fluoroplastic, PVDF has been widely studied owing to its remarkable mechanical properties, thermal stability, piezoelectric properties, in combination with good resistance to high temperatures, UV irradiation and aggressive chemicals.[25,26] Incorporation of other types of fillers into PVDF matrix has been studied with the objective to improve its properties, such as mechanical and thermal properties. Incorporation of graphite in PVDF might act as a nucleating agent and accelerated the overall non-isothermal crystallization process of PVDF. The storage modulus and the dielectric constant of the composites increased linearly with graphite concentration.[27]

The mobility of the polymer chains is restricted to some extent due to filler-polymer interaction, depending on a type of the polymers and fillers, and fillers distance which is mainly controlled by the specific surface area and filler loading.[28] The amount of immobilized rubber increases with the increasing content of CB. Stronger polymer-filler interaction would result in a thicker rubber shell for small particle-sized CB which is in combination with a larger interfacial area in the unit volume

compound at the same loading. This gives more immobilized rubber shell in comparison with large particle sized CB. It is well established that the immobilized rubber content of higher structure CB is significantly higher than its low-structure counterpart. This is probably due to high structure CB is certainly related to the increased polymer-filler interfacial area and greater adsorption ability of the freshly built surface during mixing.[29]

In the rubber manufacturing industry, fillers have been used to reinforce polymer matrices to achieve required mechanical properties. As an active filler, CB is typically adopted to reinforce FKM, such as Viton A. FKM products are exposed to intense conditions, i.e. high-temperature and chemical environments, during their lifetime.[30] Accordingly, this work investigated and elucidated the effects of different CB loadings on the rheological, thermal, tensile, dynamic mechanical, and electrical properties of PVDF and FKM composites.

Experimental

Materials. Poly(vinylidene fluoride) (PVDF, Hylar 460) with excellent temperature resistance and high chemical stability was purchased from Solvay Solexis (United States). FKM (fluoroelastomer, Viton-A401C) with high compression set resistance was also purchased from DuPont (United States). MgO and $Ca(OH)_2$ are usually used as stabilizing agents (acid acceptor) for the possible generation of hydrogen fluoride by Bisphenol. Carbon black (CB, N-330) purchased from Ahvaz Carbon Black Co. (Iran).

Sample Preparation and Composition. The PVDF and FKM composites were crosslinked with the bisphenol-A vulcanization system, and the effects of CB loadings on their rheological, thermal, tensile, electrical, and dynamic mechanical properties were studied. Figure 1 shows a schematic of the composite preparation. The bisphenol cure system has the advantages of excellent processing safety, fast cures to high states, excellent final properties, and especially high-temperature compression set resistance is shown in Figure 1. The PVDF and FKM composites loaded with CB were prepared using an internal mixer (Brabender, W50EHT, Germany) with a mixing chamber capacity of 50 cm^3. Dynamically vulcanized blends were prepared with a PVDF/FKM weight ratio of 60/40. The compounding formulation is presented in Table 1. The components were mixed in the molten state at 190 °C, PVDF was melted in the mixer for 3 min at a rotor speed of 50 and 90 rpm, and the CB was added into the mixing chamber after the torque of the chamber decreased (i.e., until a final stable torque was reached). Mixing was continued for 2 min, after which the FKM was added into the mixture. After 6 min curing was completed, the materials were collected at the end of

Table1. Formulation and Sample Codes of PVDF/FKM/CB Composites (weight ratio)

CB (phr)	FKM	PVDF	Sample
0	0	100	P
0	100	0	F
0	40	60	PF640
5	40	60	PFCB5
10	40	60	PFCB10
15	40	60	PFCB15
20	40	60	PFCB20

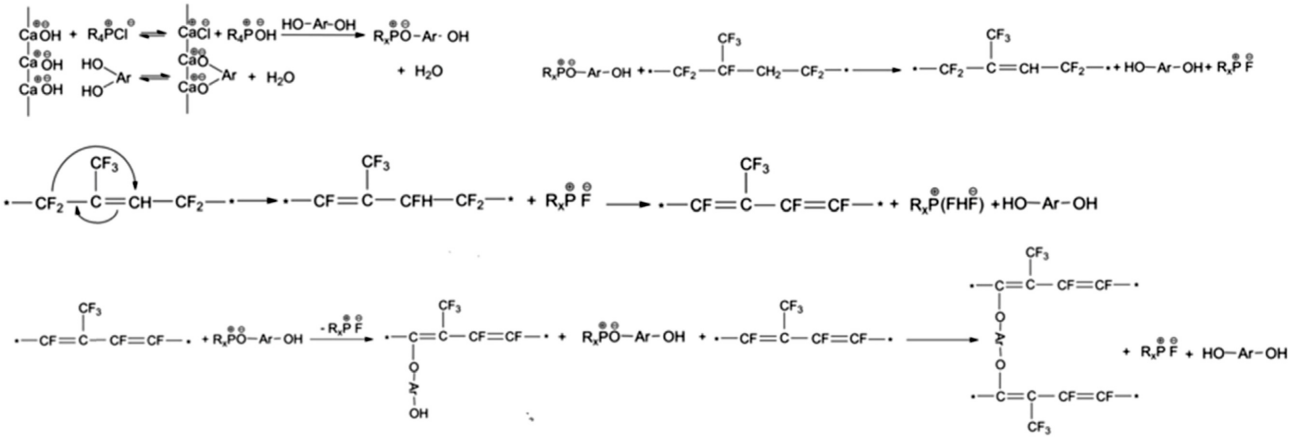

Figure 1. Mechanism for cross-linking reaction of PVDF/FKM/CB composites.

the mixing cycle. The blends were removed from the mixer and cooled at room temperature. Specimens for testing were prepared by hot press molding (Toyoseiki, MP-WCH, Japan). Dynamic mechanical analysis (DMA), thermogravimetric analysis (TGA), and differential scanning calorimetry (DSC) were then carried out to investigate the tensile, thermal, dynamic mechanical, electrical, and rheological properties of the blends.

Composites Characterization. DSC: Melting and crystallization of the composites were measured in nitrogen atmosphere using a differential scanning calorimeter (Perkin Elmer, Pyris, United Kingdom). For each test, a 5-6 mg sample was first heated to 250 °C at a rate of 10 °C/min and was then kept at this temperature for 5 min to eliminate previous thermal history. Then the sample was cooled to room temperature at a cooling rate of 20 °C/min and secondly reheated to 250 °C at the same heating rate (ASTM D3418).

TGA: A thermogravimeter (Perkin Elmer, Pyris, United Kingdom) was used to measure the weight loss of the blends under nitrogen atmosphere. The samples were heated from ambient temperature up to 600 °C at a heating rate of 20 °C/min approximately 10 mg of samples were used for each thermogravimetric analysis.

Tensile: The purpose of the tensile tests is to determine the breaking strength and elongation at break of a material. Standard tensile tests were conducted on dumbbell shaped specimens using a universal testing instrument (GoTech, China) with a tensile mode at room temperature. Test speed was kept at 50 mm/min, according to ASTM D638. All the above tests were repeated on at least five test pieces, and the results averaged.

DMA: The dynamic mechanical behavior of the composites was determined by using a dynamic mechanical analyzer (Triton, United Kingdom) with three-point bending mode at 10 Hz with a heating rate of 5 °C/min from 2150 to 80 °C. The samples were prepared as a cut strip with the size of 30, 36, and 34 mm according to ASTM E1640.

Electrical Properties: The electrical conductivity (σ) of the composites was measured using a digital high resistance meter (6517A, Keithley, USA). The resistance or conductance of a material specimen or of a capacitor is determined from a measurement of current or of voltage drop under specified conditions. By using the appropriate electrode systems, surface and volume resistance or conductance may be measured separately.

Morphology: The morphology was characterized with scanning electron microscopy (SEM) (TESCAN Co, Germany) test. The compression-molded samples were frozen in liquid nitrogen for 30 min and then cryogenically fractured in liquid nitrogen. The fractured surfaces were sputtered with gold before observation to avoid charge accumulation.

Rheological: Rheological properties of the blends were investigated using a rheometric mechanical spectrometer (RMS) equipped with parallel plate geometry (diameter=25 mm, gap=1 mm). The frequency sweep tests were performed in the range of 0.1-600 s^{-1} at temperature of 180 °C and with amplitude of 3% in order to maintain the response of materials in a linear viscoelastic regime.

Results and Discussion

Thermal Analysis. The thermal stability of the dynamically vulcanized CB-filled PVDF and FKM composites can be evaluated through TGA on the basis of nitrogen weight loss. Figure 2 and Table 2 show the thermogravimetric curves and thermal degradation data of the composites, respectively. As indicated in Figure 2, the thermograms of the neat PVDF and PF640 showed a typical single-degradation step profile. The main PVDF degradation occurred between 450 and 500 °C, indicating excellent thermal stability, whereas the main FKM

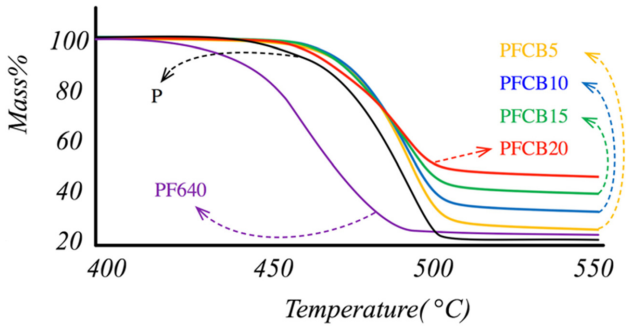

Figure 2. TGA curves of PVDF/FKM/CB composites.

Table 2. TGA Parameters for PVDF/FKM/CB Composites

Sample	Temperatures at 10% weight loss (°C)	Mass of residual composites (%)
P	456	20.5
PF640	439	23.2
PFCB5	473	26.6
PFCB10	474	33.1
PFCB15	474	39.3
PFCB20	471	46.1

degradation occurred between 350 and 470 °C.

The initiation of degradation ($T_{10\%}$) in the pristine PVDF and FKM occurred at around 439 °C. CB incorporation into PVDF and FKM increased their initiation degradation temperatures. Such as increase in the thermal stability of CB-filled PVDF and FKM composites may be due to high thermal stability of CB and its interaction with polymer matrices by proper dispersion. These intercalated polymer chains were covered by CB particles, thereby preventing the direct exposure of the chains to thermal influence.

DSC. The major heat-induced changes in the DSC thermograms of the composites at heating rate of 10 °C/min^{-1} are illustrated in Figure 3. The melting temperatures of the CB-filled PVDF and FKM composites increased as the result of CB loading. At CB loading of 5 phr, the melting temperature (Tm) increased to 173.1 °C due to the nucleation effect, but at CB loadings of 10, 15, and 20 phr, Tm slightly decreased. This finding can be attributed to CB aggregation, which increased the viscosity of the blends giving rise to poor flowability of FKM. Such flowability could be due to the rubber-filler interaction.

Table 3 presents the effects of CB grades on glass transition temperature (T_g), melting heat enthalpy (ΔH_c), and degree of crystallinity (X_c), as determined from the DSC thermograms. Generally, the incorporation of CB into crystalline polymers can significantly affect their crystallization behaviors, depending on CB dispersion and content.

The non-isothermal crystallization curves and behaviors of the CB-filled PVDF and FKM composites are shown in Figure 4. The crystallinity levels of the composites were calculated

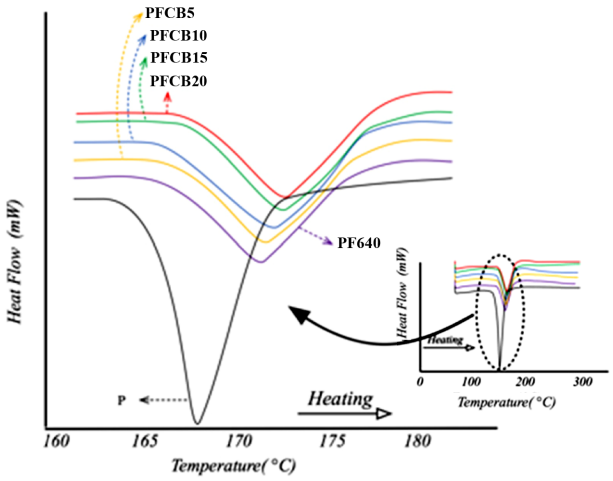

Figure 3. Melting curves of composites with different CB loading.

Table 3. The Crystallization Peak Temperature (T_c), the Melting Temperature (T_m), Melting Enthalpy (ΔH_c) and Crystallinity (X_c) of Composites

Sample	T_m(°C)	T_c (°C)	ΔH_c (J/g)	X_c (%)
P	166.6	139.1	53.61	51.2
PF640	172.4	137.6	25.2	40.1
PFCB5	173.1	138.3	25.1	39.9
PFCB10	172.9	138.4	24.9	39.7
PFCB15	172.5	138.7	24.7	39.6
PFCB20	172.1	138.8	24.6	39.5

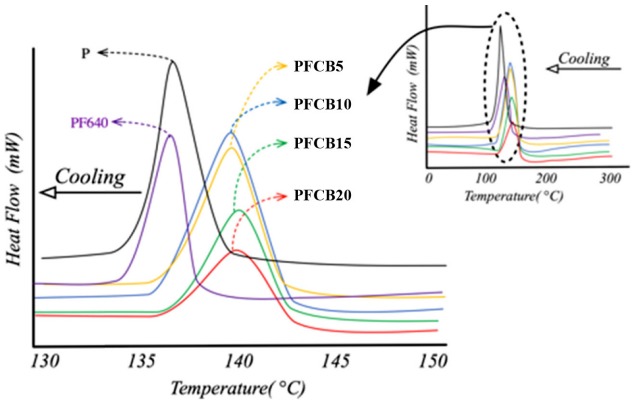

Figure 4. Crystallization curves of PVDF/FKM/CB composites of different CB loading (cooling rate V_c=10 °C min^{-1}).

using eq. (1):

$$X_c = \frac{\Delta H_c^*}{\Delta H_c \varphi} \times 100\% \quad (1)$$

where ΔH_c^*=104.7 J/g denotes the melting heat enthalpy of a 100% crystalline PVDF, φ is the PVDF content in the CB-filled PVDF and FKM composites, and ΔH_c represents the melting heat enthalpy of the DSC-measured PVDF. The related data are summarized in Table 4.

As shown in Figure 4, the crystallization peak is visibly sharpened, indicating the effective heterogeneous nucleation effect of CB. This finding accords with the previously reported results. The crystallization peak temperatures (T_c) of the composites increased with increasing CB content, but this increase slowed down at high loadings, indicating the constraining effect of CB on the motion of PVDF chains during crystallization. Such movement was constrained since FKM composite was filled with a considerable amount of CB. Conversely, the crystallinity of the CB-filled PVDF and FKM

Table 4. Tensile Properties of PVDF/FKM/CB Composites with Different CB Loading

Sample	Modulus (MPa)	Elongation-at-break (%)	Tensile strength (MPa)
PFCB5	30.2 (±0.1)	78.5(±0.1)	23.8(±0.6)
PFCB10	70.4(±0.1)	37.2(±0.2)	23.1(±0.3)
PFCB15	117.8(±0.2)	15.6(±0.2)	22.4(±0.4)
PFCB20	161.4(±0.3)	8.9(±0.3)	21.9(±0.6)
PF640	3.7(±0.3)	83.6(±0.4)	21.2(±0.5)
P	12.3(±0.1)	13.5(±0.1)	51.5(±0.7)
F	0.01(±0.002)	259(±1.4)	6.3(±0.4)

composites initially decreased with increasing CB loading. Well-dispersed CB can offer a higher number of nucleating sites and contribute in increase of the T_c. Therefore, the nucleation effect seems to dominate even when the network is formed.

Mechanical Properties. The stress–strain curves of the CB-filled PVDF and FKM composites are shown in Figure 6. The mechanical properties of the composites improved with the addition of CB, and the elongations at break decreased. The mechanical properties, such as the Young's moduli, tensile strengths, and elongations at break, of the CB-filled PVDF and FKM composites are summarized in Table 4.

Enhancement in the tensile strengths of the composites can be attributed to high degree of reinforcement induced by CB particles incorporation into the polymer matrices. Moreover, the specific surface area of CB provides the possibility for physical absorption of the polymer chain units onto its surface. The filler particles were thus covered by a semi-rigid interface, which can be considered a multifunctional physical crosslink (Figure 5). However, a further increase in CB content diminished tensile strength due to high degree of restriction, high crosslink density, and minimal mobility of the polymer chains.

As indicated in Figure 5, the CB-filled PVDF and FKM composites showed a decreasing trend in elongations at break by increase of CB loading. This is a typical phenomenon occurring when particulate fillers are incorporated into the matrices of thermoplastic vulcanizates (TPVs) and can be attributed to the greater degree of restricted chains and crosslink densities in composites embedded in molecular chains because of deformation. The elongations at break of the composites also gradually decreased because of the numerous rubber chains attached to the surface of the CB particles. The high surface area of CB led to increased interfacial interaction;

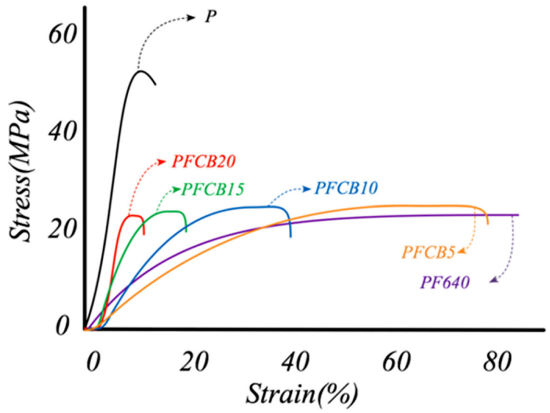

Figure 5. Tensile stress-strain curves for PVDF/FKM/CB composites with different CB loading.

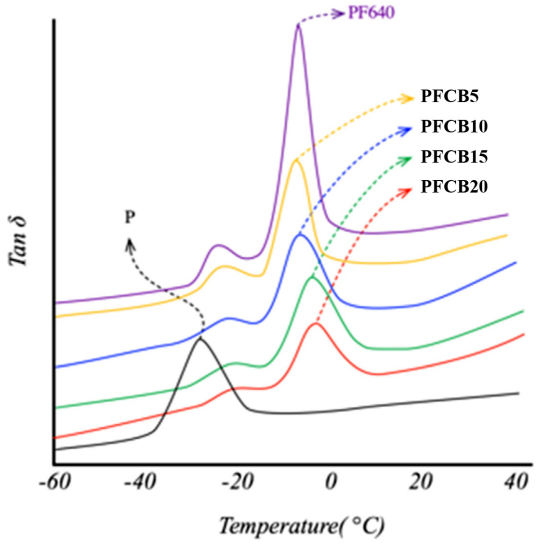

Figure 6. The tanδ profiles for PVDF/FKM/CB composites with different CB loading.

therefore, the CB particles which were locked in the rubber matrices will be more rigid than other particles (Figure 5).

Both variables increased with enhancement of CB loading as a consequence of the restriction on chain mobility at the CB surface. Such restriction, in turn, increased the stiffness of the composites. This result may again be attributed to the structural properties and high surface area of CB particles.

DMA. The effects of CB loading on the dynamic properties, namely, the loss tangents (tanδ), of the CB-filled PVDF and FKM composites are shown in Figure 6 as a function of temperature. Addition of CB increased tanδ in the tested temperature range because of the restricted movement of rubber molecules on CB surface. This movement plays a key role in the

Table 5. Tanδ Peak Temperature of the FKM and PVDF Phase in Composites with Different CB Loading

	Tanδ	
Sample	PVDF Phase	FKM Phase
P	-29	-
F	-	-5
PF640	-25.2	-3.5
PFCB5	-24.7	-3.1
PFCB10	-24.1	-2.7
PFCB15	-23.5	-2.1
PFCB20	-22.8	-1.6

reinforcement of CB. The tanδ peak emerged at around -3.5 °C, which can be ascribed to the relaxation or T_g of FKM. The storage moduli (G') of the composites sharply increased at CB loading range of 5-20 phr.

The tanδ and temperature curves reflected two separate peaks with increasing CB content, and the height and corresponding temperature of the second peak gradually decreased and increased, respectively. The first peak temperature was around -25 °C, whereas the second peak temperature of the pristine composites was about -3.5 °C with wider distribution than the first one.

The rubber chains were restricted on the surface of the CB particles, thus decreasing the chain mobility. The chains were restricted by increase of CB content. Therefore, the chain mobilities of the composites filled with a considerable amount of CB decreased.

Increase of filler content, resulted in declined dispersion of CB in FKM phase with generation of agglomerates. This phenomenon, in turn, increased the tanδ temperature of the rubber phase. The adsorption of rubber on the surface of CB was expected to decrease by increase of CB content. The area under the tanδ peak also decreased with CB loading within the examined temperature range. These results indicated the high interaction between the rubber chains and CB particles surface; such interaction retarded the motion of the rubber segments, thereby lengthening the rubber response time toward dynamic stress fields.

Electrical Properties. The logarithmic plots of conductivity (logσ) against CB loading in the CB-filled PVDF and FKM composites is presented in Figure 7. The electrical conductivities of the composites increased with rising CB loading, and the composites reached to an electrical percolation. This means that at percolation, a continuous conducting wire is

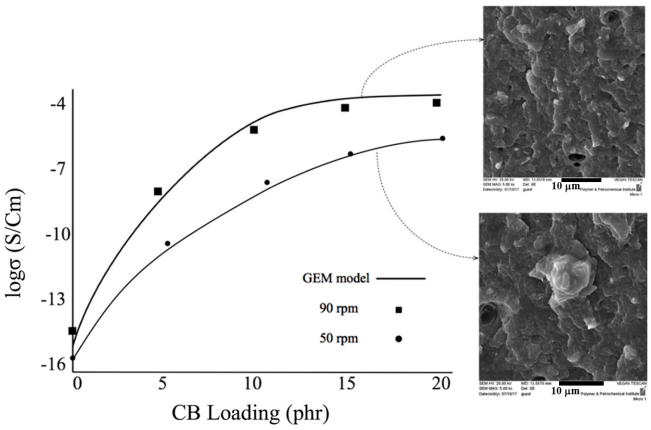

Figure 7. Electrical percolation curve for PVDF/FKM filled with the carbon black.

formed through an insulating polymer matrix, thereby transforming the polymer into a conductive substance. Beyond percolation, only an increase in the number of such wires occurs.

The general equation model (GEM) proposed by McLachlan is used to model real binary systems. The author put forward this model for conductive particles in an insulating matrix, which is the type of system studied in the current research. The model factors into the calculation of the conductivities of constituent materials, the percolation threshold, and a critical exponent. The GEM equation may also be used to measure the other physical properties (e.g., Young's modulus and thermal conductivity) of composites aside from electrical conductivity. With respect to electrical conductivity, the GEM equation is written as

$$(1-\varphi)\frac{\sigma_i^{1/s}-\sigma_m^{1/s}}{\sigma_i^{1/s}-A\sigma_m^{1/s}}+\varphi\frac{\sigma_c^{1/t}-\sigma_m^{1/t}}{\sigma_c^{1/t}-A\sigma_m^{1/t}}=0 \quad (2)$$

with $A=(1-\varphi_c)/\varphi_c$.

In this equation, σ_m is the composite conductivity, φ_c denotes the filler conductivity, φ represents the volume fraction, φ_c is the critical volume fraction of the high conductivity component at which percolation transition occurs, and t refers to the critical exponent. The GEM does not completely accurately determine the percolation threshold, but it has become the basis of many later conductivity models. Newer models have maintained a form similar to that of the GEM but use different means of solving exponent t. These models are therefore slightly more accurate predictors of electrical conductivity.[30,31]

Exponents s and t best describe the experimental results for percolation systems, especially with respect to second-order

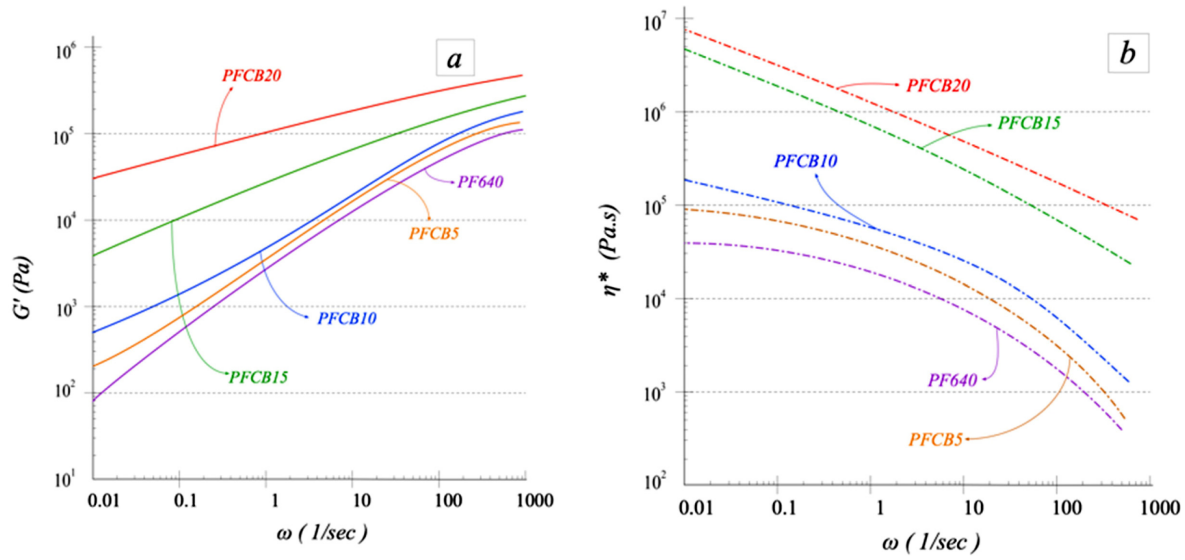

Figure 8. (a) Storage modulus (G'); (b) complex viscosity (η^*) *versus* frequency curves for PVDF/FKM/CB composites at 180 °C.

terms. When $s = t = 1$ and $\varphi_c = 1/3$, the equation is equivalent to Bruggeman's symmetric media equation. Exponent t and φ_c are related to the geometries and orientations of both components according to the following equations:

$$\varphi_c = m_f/(m_f + m_\varphi) \quad (3)$$

$$t = (m_f m_\varphi)/(m_f + m_\varphi) \quad (4)$$

where m_f is the exponent for a randomly oriented low-conductivity ellipsoid, and m_φ is the exponent for a randomly oriented high-conductivity ellipsoid.

A finite regular array of points and bonds was used to determine percolation concentration ($\varphi_c = 0.16$). Using computer simulation, the points and bonds of a cluster could be predicted. Moreover, possibility of cluster spanning the boundaries of the system could be determined.

Rheological Analysis. The rheological results are summarized in Figure 8 in terms of complex viscosity (η^*) and elastic modulus versus frequency, which also shows G' and η^* as functions of frequency for CB-filled PVDF and FKM composites. Both G' and loss moduli of the composites exhibited an increasing trend with rising frequency. For all the samples, a power law behavior was observed at low frequency in G'' with exponents smaller than 1. CB increased the viscosity levels of the composites, especially at low frequency.

This result may be ascribed to the proper interaction and entanglement between the matrix chains and CB particles and the uniform dispersion of CB in the matrices. It also indicates the existence of yield stress or, at least, the existence of very long relaxation times. When CB loading was increased, the Newtonian region weakened and disappeared from PFCB5. The complex viscosity slightly increased with CB enhancement, and PFCB20 composite exhibited a visibly higher value of $|\eta^*|$ compared with the other samples. Generally, homopolymer chains can be fully relaxed at low frequencies, but the power for the dependence of G' on frequency is usually lower than its theoretical values. Viscoelastic behavior is also considerably dependent on CB dispersion in the matrix. The relative G', which is the ratio of composite G' at a low frequency to that of PF460, is a valuable parameter for describing the rheological percolation of the composites. In this work, G' and G'' values decreased over the entire range of frequencies.

Conclusions

The dynamic mechanical, electrical, thermal, tensile, and rheological properties of CB-filled PVDF and FKM composites were investigated in this research. Enhanced tensile properties were observed in the composites, with the maximum tensile strength obtained at CB loading of 20 phr. However, the elongations at break decreased with increase of CB loading, which significantly enhanced the Young's moduli of the composites. The DMA analysis revealed a significant improvement in the G' and a reduction in the tanδ peak heights of the composites, which were due to high reinforcement efficiency of CB particles. The enhanced thermal stability levels

of the composites may be attributed to the high thermal stability of CB and its interaction with the polymer matrix. T_c of the composites increased as a result of well-dispersed CB and generation of more nucleating sites. The abrupt increase in Young's moduli and G' values by addition of CB content greater than 20 phr could be assigned to electrical percolation.

References

1. A. Fina, Z. Han, G. Saracco, and U. Gross, *Polym. Adv. Technol.*, **23**, 1572 (2012).
2. K. P. Pramoda, N. T. T. Linh, P. S. Tang, and W. C. Tjiu, *Compos. Sci. Technol.*, **70**, 578 (2010).
3. E. Sharifzadeh, I. Ghasemi, M. Karrabi, and H. Azizi, *Iran. Polym. J.*, **23**, 525 (2014).
4. N. Wang, P. R. Chang, P. Zheng, and X. Ma, *Appl. Surf. Sci*., **314**, 815 (2014).
5. Y. Y. Shi, J. H. Yang, T. Huang, N. Zhang, and C. Chen, *Composites Part B*, **55**, 463 (2013).
6. J. Varga and A. Menyhárd, *J. Therm. Anal. Calorim.*, **73**, 735 (2003).
7. H. Ma, Z. Xiong, F. Lv, C. Li, and Y. Yang, *Macromol. Mater. Eng.*, **297**, 136 (2012).
8. H. Ma, Z. Xiong, F. Lv, C. Li, and Y. Yang, *Macromol. Chem. Phys.*, **212**, 252 (2011).
9. C. Zhao, X. Xu, J. Chen, G. Wang, and F. Yang, *Desalination*, **340**, 59 (2014).
10. E. Kalkornsurapranee, C. Nakason, C. Kummerlöwe, and N. Vennemann, *J. Appl. Polym. Sci.*, **128**, 2358 (2013).
11. S. Mani, P. Cassagnau, M. Bousmina, and P. Chaumont, *Macromol. Mater. Eng*., **296**, 909 (2011).
12. C. Xu, Y. Wang, and Y. Chen, *Polym. Test.*, **33**, 179 (2014).
13. Y. Wang, L. Fang, C. Xu, Z. Chen, and Y. Chen, *Polym. Test.*, **32**, 1072 (2013).
14. S. Mohamadi and N. Sharifi-Sanjani, *Polym. Compos*., **32**, 1451 (2011).
15. S. H. Lin, C. F. Hsieh, M. H. Li, and K. L. Tung, *Desalination*, **249**, 647 (2009).
16. A. S. Bhatt, D. K. Bhat, and M. S. Santosh, *J. Appl. Polym. Sci*., **119**, 968 (2011).
17. Z. Major and R. W. Lang, *Eng. Fail. Anal*., **17**, 701 (2010).
18. N. Hinchiranan, P. Wannako, B. Paosawatyanyong, and P. Prasassarakich, *Mater. Chem. Phys*., **139**, 689 (2013).
19. S. H. Lee, S. S. Yoo, D. E. Kim, B. S. Kang, and H. E. Kim, *Polym., Test.*, **31**, 993 (2012).
20. Y. Wang, X. Jiang, Z. Chen, and Y. Chen, *Polym. Test.*, **32**, 1392 (2013).
21. B. Hu, N. Hu, L. Wu, H. Cui, and J. Ying, *Funct. Mater. Lett*., **8**, 234 (2015).
22. M. J. Lacey, F. Jeschull, K. Edström, and D. Brandell, *J. Am. Chem. Soc.*, **118**, 25890 (2014).
23. M. Litvinov, R. A. Orza, M. Klüppel, M. Van Duin, and M. Magusin, *Macromolecules*, **44**, 4887 (2011).
24. N. J. S. Sohi, S. Bhadra, and Khastgir, *Carbon*, **49**, 1349 (2011).
25. M. M. Abolhasani, A. Jalali-Arani, H. Nazockdast, and Q. Guo, *Polymer*, **54**, 4686 (2013).
26. K. Ke, Y. Wang, W. Yang, B. H. Xie, and M. B. Yang, *Polym. Test*., **31**, 117 (2012).
27. M. Scott, T. Parsons, M. Nevell, and S. Perera, *J. Appl. Polym. Sci*., **120**, 3673 (2011).
28. L. Wu, W. Yuan, N. Hu, Z. Wang, C. Chen, J. Qiu, J. Ying, and Y. Li, *J. Appl. Phys.*, **47**, 276 (2014).
29. C. Baudouin and C. Bailly, *Polym. Degrad. Stab.*, **95**, 389 (2010).
30. R. Ram, M. Rahaman, and D. Khastgir, *Composites Part A,* **69**, 30 (2015).
31. J. Xia, Y. Pan, and L. Shen, *J. Mater. Sci*., **35**, 6145 (2000).